

**SYNTHESIS OF BIFUNCTIONAL ACTIVATED
CARBON FROM GASIFICATION RESIDUES FOR
MALACHITE GREEN DYE AND ATENOLOL
ADSORPTION**

ANIS ATIKAH BINTI AHMAD

UNIVERSITI SAINS MALAYSIA

2020

**SYNTHESIS OF BIFUNCTIONAL ACTIVATED
CARBON FROM GASIFICATION RESIDUES FOR
MALACHITE GREEN DYE AND ATENOLOL
ADSORPTION**

by

ANIS ATIKAH BINTI AHMAD

**Thesis submitted in fulfilment of the requirements
for the degree of
Doctor of Philosophy**

September 2020

ACKNOWLEDGEMENT

Alhamdulillah. Praise to Allah and thanks to Him, this work is successfully completed on time. Many different groups of people collectively played a part in completing this report directly or indirectly. Therefore, I would like to take this opportunity to pay tribute to all of them.

I wish to place on record the appreciation to my parents, husband and family for their endless prayers and supports. Without their prayers, I might not be able to successfully complete this project on time.

Special thanks go to Prof Dr Mohd Azmier bin Ahmad and Dr Azam Taufik Mohd Din for their invaluable guidance and worthy contributions as a supervisor and co-supervisor from the beginning until the end of the study period. Their constant support to me in completing this project is really appreciated. I wish every success in their upcoming endeavours.

I extend my utmost gratitude to all technicians of School of Chemical Engineering, Universiti Sains Malaysia for their precious cooperation and support in assisting me with the lab works. Sincere appreciation also goes to all friends for being very helpful and ready to help at any time.

I also would like to thank Universiti Malaysia Perlis and Ministry of Higher Education for their financial support throughout this program. The funding provided by USM under University Grant (1001/PJKIMIA/8014061 and 1001/PJKIMIA/6316195) and External Grant from NAHRIM (304/PJKIMIA/6050434/I136) for conducting the research work are gratefully acknowledged. Last but not least, thanks to all persons who are directly or indirectly involved in giving their helpful hands during these 3 years of study.

TABLE OF CONTENTS

ACKNOWLEDGEMENT	ii
TABLE OF CONTENTS	iii
LIST OF TABLES	viii
LIST OF FIGURES	xii
LIST OF SYMBOLS & UNITS	xviii
LIST OF ABBREVIATIONS	xxi
ABSTRAK	xxiii
ABSTRACT	xxv
CHAPTER 1 INTRODUCTION	1
1.1 Background of Study.....	1
1.1.1 Malachite Green	2
1.1.2 Atenolol	2
1.1.3 Activated Carbon.....	3
1.1.4 Gasification Char Residues	5
1.1.5 Microwave Activation Technology	6
1.2 Problem Statement	6
1.3 Research Objectives	9
1.4 Scope of Study	10
1.5 Gap of knowledge	11
1.6 Thesis Outline	11
CHAPTER 2 LITERATURE REVIEW	13
2.1 Introduction	13
2.2 Adsorption.....	13
2.3 Gasification Char Residues as a Precursor for AC Production.....	15

2.3.1	Physical Properties	16
2.3.2	Chemical Properties.....	18
2.3.3	Recent Studies on Adsorption Using GC	22
2.4	AC Production.....	24
2.5	MW Activation Techniques	28
2.5.1	Effect of Radiation Power (RP).....	31
2.5.2	Effect of Radiation Time (RT)	33
2.5.3	Effect of Impregnation Ratio (IR)	34
2.6	Optimization of AC Preparation Condition	36
2.7	Batch Adsorption Study	37
2.7.1	Effect of Initial Concentration and Contact Time	37
2.7.2	Effect of Temperature.....	39
2.7.3	Effect of pH	40
2.8	Adsorption Isotherm and Kinetic	41
2.9	Adsorption Mechanism and Interactions.....	47
2.10	Adsorption Thermodynamics	48
2.11	Fixed-Bed Column Study	52
2.11.1	Dynamic Modelling of Breakthrough Curve.....	57
2.12	Conclusion.....	60
CHAPTER 3 METHODOLOGY		61
3.1	Introduction	61
3.2	Experimental Overview.....	61
3.3	Materials.....	63
3.4	Equipment and Instrumentations.....	65
3.4.1	AC Preparation System	65
3.4.2	Characterization System	67

3.4.2(a)	Micromeritics Accelerated Surface Area and Porosity Analyzer	67
3.4.2(b)	Thermogravimetric Analyzer.....	67
3.4.2(c)	Elemental Analyzer.....	61
3.4.2(d)	Scanning Electron Microscopy	68
3.4.2(e)	Fourier Transform Infrared (FTIR) Spectroscopy	68
3.4.3	Batch Adsorption System	69
3.4.4	Fixed-Bed Column Adsorption System.....	69
3.4.5	Analysis System	71
3.5	Experimental Procedure	71
3.5.1	AC Preparation	71
3.5.2	Optimization of Activation Condition.....	72
3.5.3	Parametric Study of Batch Adsorption.....	74
3.5.3(a)	Effect of Contact Time and Initial Concentration.....	75
3.5.3(b)	Effect of Solution Temperature	75
3.5.3(c)	Effect of Initial Solution pH.....	75
3.5.4	Fitting of Adsorption Isotherm Model.....	76
3.5.5	Fitting of Adsorption Kinetic Model	78
3.5.6	Rate-Limiting Steps of Adsorption.....	79
3.5.7	Thermodynamic Study	80
3.5.8	Fixed-Bed Colum Adsorption Study	81
CHAPTER 4	RESULTS AND DISCUSSIONS.....	83
4.1	Experimental Design	83
4.1.1	Regression Model Development of GOPEFBAC	83
4.1.2	3D Surface Plot of GOPEFBAC	88
4.1.3	Regression Model Development of GRTRAC.....	91
4.1.4	3D Surface Plot of GOPEFBAC	95
4.1.5	Regression Model Development of GGSWAC.....	98

4.1.6	3D Surface Plot of GGSWAC	103
4.1.7	Comparison of GOPEFBAC, GRTRAC & GGSWAC Performance	104
	4.1.7(a) Interpretation of Regression Analysis	104
	4.1.7(b) 3D Surface Plot	106
	4.1.7(c) Optimization and Validation	107
4.2	Characterization of GCs and ACs	108
4.2.1	Surface Area and Pore Properties	108
4.2.2	Proximate and Elemental Analysis	113
4.2.3	Surface Morphology	116
4.2.4	Surface Chemistry	116
4.3	Batch Adsorption Study	121
4.3.1	Equilibrium Study	121
	4.3.1(a) Effect of Contact Time & Initial Concentration	121
	4.3.1(b) Effect of Solution Temperature	122
	4.3.1(c) Effect of Initial Solution pH	126
4.3.2	Isotherm Study	129
4.3.3	Kinetic Study	145
4.3.4	Rate-Limiting Steps of Adsorption	159
	4.3.4(a) Weber-Morris Intraparticle Diffusion Model	159
	4.3.4(b) Boyd Model	164
	4.3.4(c) Diffusion-Chemisorption Model	167
4.4	Thermodynamic Study	169
4.5	Mechanism of ACs Adsorption	173
4.6	Summary on ACs Performace in Batch Study	177
4.7	Fixed-Bed Column Study	178
4.7.1	Effect of Influent Concentration	178
4.7.2	Effect of Influent Flow Rate	181

4.7.3	Effect of Bed Depth.....	184
4.7.4	Comparison on Overall ACs Performance for MG and ATN Adsorption	184
4.7.5	Dynamic Modelling of Breakthrough Curve.....	188
CHAPTER 5 CONCLUSION AND RECOMMENDATIONS.....		193
5.1	Conclusion.....	193
5.2	Recommendations	195
REFERENCES		197
APPENDICES		
Appendix A Microwave Power Calculation		
Appendix B Calibration Curve		
Appendix C Elemental Analysis		
Appendix D Plots of Adsorption Uptakes versus Time		
Appendix E Parameters of Kinetics		
Appendix F Intraparticle Model Plots		
Appendix G Boyd Plots		
Appendix H Thermodynamic Plot		
LIST OF PUBLICATIONS		

LIST OF TABLES

	Page
Table 2.1 Advantages and disadvantages of various pollutant removal technologies (Zhou et al., 2019).....	14
Table 2.2 Physical characteristic of GC residues.....	19
Table 2.3 Chemical properties of GC.....	22
Table 2.4 GC in adsorption applications.....	25
Table 2.5 Various activation methods for AC production.....	29
Table 2.6 Optimization parameter of different adsorbent for dyes and pharmaceuticals removal.....	38
Table 2.7 Effect of temperature on MG adsorption.....	39
Table 2.8 Effect of temperature on ATN adsorption.....	40
Table 2.9 Optimum pH for MG adsorption.....	41
Table 2.10 Optimum pH for ATN adsorption.....	41
Table 2.11 Isotherm & Kinetic Model of MG.....	45
Table 2.12 Isotherm & Kinetic Model of ATN.....	46
Table 2.13 Mechanism of MG adsorption.....	49
Table 2.14 Mechanism of ATN adsorption.....	50
Table 2.15 Thermodynamic parameters for adsorption of MG on various low-cost adsorbents.....	53
Table 2.16 Thermodynamic parameters for adsorption of atenolol on various adsorbents.....	56
Table 2.17 Dynamic modelling of breakthrough curve.....	59
Table 2.18 Adopted literature.....	60
Table 3.1 List of reagents and chemicals.....	63
Table 3.2 Properties of MG.....	64

Table 3.3	Properties of ATN	64
Table 3.4	Complete design matrix for AC preparation	73
Table 4.1	Experimental design matrix for preparation of GOPEFBAC	84
Table 4.2	ANOVA and lack of fit test for response surface quadratic model for MG removal of GOPEFBAC	87
Table 4.3	ANOVA and lack of fit test for response surface quadratic model for ATN removal of GOPEFBAC	88
Table 4.4	ANOVA and lack of fit test for response surface quadratic model for GOPEFBAC yield	89
Table 4.5	Experimental design matrix for preparation of GRTRAC	92
Table 4.6	ANOVA and lack of fit test for response surface quadratic model for MG removal of GRTRAC	94
Table 4.7	ANOVA and lack of fit test for response surface quadratic model for ATN removal of GRTRAC	95
Table 4.8	ANOVA and lack of fit test for response surface quadratic model for GRTRAC yield	96
Table 4.9	Experimental design matrix for preparation of GGSWAC	98
Table 4.10	ANOVA and lack of fit test for response surface quadratic model for MG removal of GGSWAC	101
Table 4.11	ANOVA and lack of fit test for response surface quadratic model for ATN removal of GGSWAC	102
Table 4.12	ANOVA and lack of fit test for response surface quadratic model for GGSWAC yield	102
Table 4.13	Significant factor for GOPEFBAC, GRTRAC and GGSWAC from ANOVA	105
Table 4.14	Model validation for ACs prepared for MG removal and yield	109
Table 4.15	Model validation for AC prepared for ATN removal and yield	109
Table 4.16	Surface area and pore characteristics of the samples	111

Table 4.17	Optimum pH for MG adsorption	127
Table 4.18	Optimum pH for ATN adsorption.....	129
Table 4.19	Isotherm parameters for adsorption of MG dyes by optimized GOPEFBAC, GRTRAC and GGSWAC at 30, 45 and 60 °C.....	138
Table 4.20	Isotherm parameters for adsorption of ATN by optimized GOPEFBAC, GRTRAC and GGSWAC at 30, 45 and 60°C.....	141
Table 4.21	Kinetic parameters for MG-GOPEFBAC, MG-GRTRAC and MG- GGSWAC systems at 30 °C.....	155
Table 4.22	Kinetic parameters for ATN-GOPEFBAC, ATN-GRTRAC and ATN-GGSWAC systems at 30 °C	157
Table 4.23	Intraparticle diffusion model constant and R ² values for adsorption of MG-GOPEFBAC, MG-GRTRAC and MG-GGSWAC at 30 °C	162
Table 4.24	Intraparticle diffusion model constant and R ² values for adsorption of ATN-GOPEFBAC, ATN-GRTRAC and ATN-GGSWAC at 30 °C	163
Table 4.25	Boyd plot diffusion coefficients of MG adsorption onto GOPEFBAC, GRTRAC and GGSWAC at 30 °C	167
Table 4.26	Boyd plot diffusion coefficients of ATN adsorption onto GOPEFBAC, GRTRAC and GGSWAC at 30 °C	167
Table 4.27	Thermodynamic parameters for MG adsorption onto optimized ACs.....	170
Table 4.28	Thermodynamic parameters for ATN adsorption onto optimized ACs.....	171
Table 4.29	Summary of the type of adsorption for GOPEFBAC, GRTRAC, GGSWAC on MG and ATN adsorption	179
Table 4.30	Column data parameters for adsorption of MG onto GOPEFBAC, GRTRAC and GGSWAC	188
Table 4.31	Column data parameters for adsorption of ATN onto GOPEFBAC, GRTRAC and GGSWAC	189

Table 4.32	Comparison on performance of batch and column study.....	189
Table 4.33	Parameters predicted from the Adams-Bohart model for MG and ATN adsorption by GOPEFBAC, GRTRAC and GGSWAC	190
Table 4.34	Parameters predicted from the Yoon-Nelson model for MG and ATN adsorption by GOPEFBAC, GRTRAC and GGSWAC	191
Table 4.35	Parameters predicted from the Adams-Bohart model for MG and ATN adsorption by GOPEFBAC, GRTRAC and GGSWAC	191

LIST OF FIGURES

	Page
Figure 1.1	U.S. AC Demand 2014-2025 (Grand View Research, 2019)4
Figure 1.2	Global end use of AC (Grand View Research, 2019).....5
Figure 3.1	Schematic flow diagram of experimental activities62
Figure 3.2	Woodchip gasification waste from (a) GOPEFB (b) GRTR and (c) GGSW63
Figure 3.3	Image of the microwave activation unit.....65
Figure 3.4	Process flow diagram (PFD) of the microwave activation unit66
Figure 3.5	Process flow diagram (PFD) of adsorption column system.....70
Figure 4.1	Predicted versus actual experimental values for (a) MG removal, (b) ATN removal and (c) GOPEFBAC yield.....86
Figure 4.2	3D response plot for (a) MG removal (effect of radiation power and IR, radiation time = 1 min), (b) ATN removal (effect of radiation power and IR, radiation time = 1 min) and (c) GOPEFBAC yield (effect of radiation power and radiation time, IR = 0.5)90
Figure 4.3	Predicted versus actual experimental values for (a) MG removal, (b) ATN removal and (c) GRTRAC yield93
Figure 4.4	3D response plot for (a) MG removal (effect of radiation power and IR, radiation time = 1 min), (b) ATN removal (effect of radiation power and IR, radiation time = 1 min) and (c) GRTRAC yield (effect of radiation power and radiation time, IR = 0.5)97
Figure 4.5	Predicted versus actual experimental values for (a) MG removal, (b) ATN removal and (c) GGSWAC yield100

Figure 4.6	3D response plot for (a) MG removal (effect of radiation power and IR, radiation time = 1.0 min), (b) ATN removal (effect of radiation power and IR, radiation time = 1.0 min) and (c) GGSWAC yield (effect of radiation power and radiation time, IR = 0.5)	104
Figure 4.7	N ₂ adsorption–desorption isotherms profiles for (a) GOPEFBAC, (b) GRTRAC and (c) GGSWAC	110
Figure 4.8	Pore size distributions of (a) MG-GOPEFBAC, MG-GRTRAC and MG-GGSWAC; (b) ATN-GOPEFBAC, ATN-GRTRAC and ATN-GGSWAC	112
Figure 4.9	Proximate analysis of GOPEFBAC, GRTRAC, GGSWAC, MG-GOPEFBAC, MG-GRTRAC, MG-GGSWAC, ATN-GOPEFBAC, ATN-GRTRAC and ATN-GGSWAC	114
Figure 4.10	Elemental analysis of GOPEFBAC, GRTRAC, GGSWAC, MG-GOPEFBAC, MG-GRTRAC, MG-GGSWAC, ATN-GOPEFBAC, ATN-GRTRAC and ATN-GGSWAC	115
Figure 4.11	SEM images of (a) GOPEFB and (b) MG-GOPEFBAC (c) ATN-GOPEFBAC (magnification of 3000 x).....	117
Figure 4.12	SEM images of (a) GRTR and (b) MG-GRTRAC (c) ATN-GRTRAC (magnification of 3000 x)	117
Figure 4.13	SEM images of (a) GGSW and (b) MG-GGSWAC (c) ATN-GGSWAC (magnification of 3000 x)	117
Figure 4.14	FTIR spectrum for GOPEFB, MG-GOPEFBAC and ATN-GOPEFBAC.....	118
Figure 4.15	FTIR spectrum for GRTR, MG-GRTRAC and ATN-GRTRAC.....	119
Figure 4.16	FTIR spectrum for GGSW, MG-GGSWAC and ATN-GGSWAC .	120
Figure 4.17	MG adsorption uptake versus adsorption time at various initial concentrations by (a) MG-GOPEFBAC, (b) MG-GRTRAC and (c) MG-GGSWAC at 30 °C	123

Figure 4.18	ATN adsorption uptake versus adsorption time at various initial concentrations by (a) ATN-GOPEFBAC, (b) ATN-GRTRAC and (c) ATN-GGSWAC at 30 °C	124
Figure 4.19	Effect of solution temperature on MG adsorption capacity of MG-GOPEFBAC, MG-GRTRAC and MG-GGSWAC systems (condition: initial concentration 100 mg/L)	125
Figure 4.20	Effect of solution temperature on ATN adsorption capacity of ATN-GOPEFBAC, ATN-GRTRAC and ATN-GGSWAC systems (condition: initial concentration 100 mg/L)	126
Figure 4.21	Effect of initial pH on MG adsorption capacity of MG-GOPEFBAC, MG-GRTRAC and MG-GGSWAC systems (condition: initial concentration 100 mg/L)	127
Figure 4.22	Effect of initial pH on ATN adsorption capacity of ATN-GOPEFBAC, ATN-GRTRAC and ATN-GGSWAC systems (condition: initial concentration 100 mg/L)	128
Figure 4.23	Plots of (a) Langmuir, (b) Freundlich, (c) Temkin, (d) Dubinin-Radushkevich, (e) Sips and (f) <i>n</i> -BET for MG adsorption onto optimized GOPEFBAC at 30, 45 and 60 °C	130
Figure 4.24	Plots of (a) Langmuir, (b) Freundlich, (c) Temkin, (d) Dubinin-Radushkevich, (e) Sips and (f) <i>n</i> -BET for MG adsorption onto optimized GRTRAC at 30, 45 and 60 °C	131
Figure 4.25	Plots of (a) Langmuir, (b) Freundlich, (c) Temkin, (d) Dubinin-Radushkevich, (e) Sips and (f) <i>n</i> -BET for MG adsorption onto optimized GGSWAC at 30, 45 and 60 °C	132
Figure 4.26	Plots of (a) Langmuir, (b) Freundlich, (c) Temkin, (d) Dubinin-Radushkevich, (e) Sips and (f) <i>n</i> -BET for ATN adsorption onto optimized GOPEFBAC at 30, 45 and 60 °C	133
Figure 4.27	Plots of (a) Langmuir, (b) Freundlich, (c) Temkin, (d) Dubinin-Radushkevich, (e) Sips and (f) <i>n</i> -BET for ATN adsorption onto optimized GRTRAC at 30, 45 and 60 °C	134

Figure 4.28	Plots of (a) Langmuir, (b) Freundlich, (c) Temkin, (d) Dubinin-Radushkevich, (e) Sips and (f) <i>n</i> -BET for ATN adsorption onto optimized GGSWAC at 30, 45 and 60 °C	135
Figure 4.29	Number of layers in multilayer adsorption	136
Figure 4.30	Plots of separation factor, R_L versus MG initial concentration for optimized GOPEFBAC, GRTRAC and GGSWAC at (a) 30 °C, (b) 45 °C and (c) 60 °C	140
Figure 4.31	Plots of separation factor, R_L versus ATN initial concentration for optimized GOPEFBAC, GRTRAC and GGSWAC at (a) 30 °C, (b) 45 °C and (c) 60 °C	143
Figure 4.32	Plots of Pseudo-first order kinetic model for (a) MG- GOPEFBAC, (b)MG-GRTRAC and (c) MG-GGSWAC systems at 30 °C.....	147
Figure 4.33	Plots of Pseudo-second order kinetic model for (a) MG- GOPEFBAC, (b) MG-GRTRAC and (c) MG-GGSWAC systems at 30 °C.....	148
Figure 4.34	Plots of Elovich kinetic model for (a) MG-GOPEFBAC, (b) MG-GRTRAC and (c) MG-GGSWAC systems at 30 °C	149
Figure 4.35	Plots of Avrami kinetic model for (a) MG-GOPEFBAC, (b) MG-GRTRAC and (c) MG-GGSWAC systems at 30 °C	150
Figure 4.36	Plots of Pseudo-first order kinetic model for (a) ATN- GOPEFBAC, (b) ATN-GRTRAC and (c) ATN-GGSWAC systems at 30 °C.....	151
Figure 4.37	Plots of Pseudo-second order kinetic model for (a) ATN- GOPEFBAC, (b) ATN-GRTRAC and (c) ATN-GGSWAC systems at 30 °C.....	152
Figure 4.38	Plots of Elovich kinetic model for (a) ATN-GOPEFBAC, (b) ATN-GRTRAC and (c) ATN-GGSWAC systems at 30 °C	153
Figure 4.39	Plots of Avrami kinetic model for (a) ATN-GOPEFBAC, (b) ATN-GRTRAC and (c) ATN-GGSWAC systems at 30 °C	154

Figure 4.40	Plots of intraparticle diffusion model for MG adsorption onto (a) GOPEFBAC, (b) GRTRAC (c) GGSWAC	160
Figure 4.41	Plots of intraparticle diffusion model for ATN adsorption onto (a) GOPEFBAC, (b) GRTRAC (c) GGSWAC	161
Figure 4.42	Boyd's plots for MG adsorption onto (a) GOPEFBAC, (b) GRTRAC and (c) GGSWAC at 30 °C.....	165
Figure 4.43	Boyd's plots for ATN adsorption onto (a) GOPEFBAC, (b) GRTRAC and (c) GGSWAC at 30 °C.....	166
Figure 4.44	Chemical-diffusion plots for ATN adsorption onto (a) GOPEFBAC, (b) GRTRAC and (c) GGSWAC at 30 °C	168
Figure 4.45	Monolayer adsorption- Adsorbent-Adsorbate (MG) interactions....	174
Figure 4.46	Monolayer adsorption- Adsorbent-Adsorbate (ATN) interactions..	175
Figure 4.47	Multilayer formation- Adsorbate (MG)-adsorbate (MG) interactions	175
Figure 4.48	Multilayer formation- Adsorbate (ATN)-adsorbate (ATN) interactions	176
Figure 4.49	Adsorption mechanism steps.....	176
Figure 4.50	Breakthrough curve of MG adsorption onto (a) GOPEFBAC, (b) GRTRAC and (c) GGSWAC at different initial concentration (flowrate = 2 ml/min and bed height = 2 cm)	179
Figure 4.51	Breakthrough curve of ATN adsorption onto (a) GOPEFBAC, (b) GRTRAC and (c) GGSWAC at different initial concentration (flowrate = 2 ml/min and bed height = 2 cm)	180
Figure 4.52	Breakthrough curve of MG adsorption onto (a) GOPEFBAC, (b) GRTRAC and (c) GGSWAC at different influent flowrate (initial concentration = 100 mg/L and bed height = 2 cm)	182
Figure 4.53	Breakthrough curve of ATN adsorption onto (a) GOPEFBAC, (b) GRTRAC and (c) GGSWAC at different influent flowrate (initial concentration = 100 mg/L and bed height = 2 cm)	183

Figure 4.54 Breakthrough curve of MG adsorption onto (a) GOPEFBAC, (b) GRTRAC and (c) GGSWAC at different bed height (initial concentration = 100 mg/L and feed flowrate = 0.5 ml/min)..... 185

Figure 4.55 Breakthrough curve of ATN adsorption onto (a) GOPEFBAC, (b) GRTRAC and (c) GGSWAC at different bed height (initial concentration = 100 mg/L and feed flowrate = 0.5 ml/min))..... 186

LIST OF SYMBOLS & UNITS

Symbol	Description	Unit
b_i	Linear coefficient	-
b_0	Constant coefficient	-
b_{ii}	Quadratic coefficient	-
b_{ij}	Interaction coefficient	-
b_T	Temkin constant related to the heat of adsorption	J/mol
B	Boyd plot slope	-
B_t	Boyd plot constant	-
C	Intercept related to the boundary layer effect	mg/g
C_e	Adsorbate concentration at equilibrium	mg/L
C_0	Adsorbate concentration at initial	mg/L
C_t	Adsorbate concentration at time “t”	mg/L
C_{ad}	Adsorbed solute concentration	mg/L
D_i	Effective diffusion coefficient	m ² /h
e_i	Error	-
E_{DR}	Mean energy of sorption	kJ/mol
H	The bed depth of column	cm
k_A	Adams-Bohart kinetic constant	L/min.mg
k_{DC}	Diffusion-chemisorption rate constant	mg/g hr ^{1/2}
k_T	Temkin isotherm constant	L/g
k_{TH}	Thomas rate constant	L/min mg
k_Y	Yoon Nelson rate constant	1/min
k_{AV}	Avrami constant	1/h
k_{ii}	Intraparticle diffusion rate constant	mg/g h ^{1/2}
k_1	Pseudo-first order model rate constant	1/h
k_2	Pseudo-second order rate constant	g/mg h
K_C	The equilibrium constant	-
K_L	Langmuir model constant	L/mg
$K_{L,BET}$	Upper layer equilibrium constant	L/mg

K_S	First layer equilibrium constant	L/mg
K_{Sips}	Sips equilibrium constant	(L/mg) ^{n_s}
K_f	Freundlich constant related to adsorption capacity	(m/g)(L/mg) ^{1/n}
m_s	Dry weight of the adsorbent after exhausted	g
m_{tot}	Quantity of adsorbates deposited in the column	g
M	Mass of activated carbon	g
n	Number of variables	-
n_c	Number of centre runs	-
n_F	Freundlich constant related to sorption intensity of the sorbent	-
n_{AV}	Avrami model exponent of time	-
n_{BET}	Maximum number of adsorbed layers on the solid surface	-
n_{SIPS}	Heterogeneity exponent	-
N	Number of data points	-
N_0	Adams-Bohart saturation concentration	mg/L
q_e	Amount of adsorbate adsorbed at equilibrium	mg/g
q_{TH}	Thomas adsorption capacity of the bed	mg/g
q_t	Adsorption capacity of adsorbent at time “t”	mg/g
q_{bed}	Bed capacity	mg/g
q_{tot}	Total adsorbed quantity of adsorbate	mg
$q_{e,exp}$	Experimental amount of adsorbate adsorbed at equilibrium	mg/g
$q_{e,cal}$	Calculated amount of adsorbate adsorbed at equilibrium	mg/g
Q	Volumetric flow rate	mL/min
Q_m	Langmuir monolayer adsorption capacity	mg/g
Q_{DR}	Dubinin–Radushkevich monolayer adsorption capacity	mg/g
Q_{SIPS}	Sips maximum adsorption capacity	mg/g
r	Radius of the adsorbent particle	m
R	Perfect gas constant	J/mol.K
R_L	Langmuir adsorption isotherm characteristic	-
R^2	Correlation coefficient	-
S_{BET}	BET surface area	m ² /g
t_{tot}	Total flow time until exhaustion	min
T	Absolute temperature	K
U_o	Linear velocity	cm/min

V	Volume of the solution	L
W_{char}	Dry weight of char	g
W_{KOH}	Dry weight of KOH pellets	g
W	Mass of adsorbent	g
x_1	Radiation power	Watt
x_2	Radiation time	min
x_3	Impregnation ratio	-
Y_1	Percentage of adsorbate removal	%
Y_2	Yield percentage	%

Greek letters

$\pm\alpha$	Distance of axial point from centre	-
α_E	Elovich initial adsorption rate	mg/g min
β_E	Elovich desorption constant	g/mg
ΔG°	Change in free energy	kJ/mol
ΔH°	Change in enthalpy	kJ/mol
ΔS°	Change in entropy	kJ/mol
Δq	The normalised standard deviation	-
λ	Wavelength	nm
π	Ratio of a circle's circumference to its diameter	-
τ	Time required for 50% adsorbate breakthrough	min
χ^2	Chi-square	-

LIST OF ABBREVIATIONS

AC	Activated carbon
ANOVA	Analysis of variance
AP	Adequate Precision
APD	Average pore diameter
ATN	Atenolol
BDST	Bed depth service time
BET	Brunauer-Emmett-Teller
CCD	Central composite design
DoE	Design of experiment
DR	Dubinín–Radushkevich
FC	Fixed carbon
FR	Freundlich
FTIR	Fourier transform infrared
GC	Gasification char
GGSW	Gasified <i>Glyricidia sepium</i> wood
GGSWAC	Gasified <i>Glyricidia sepium</i> wood-based activated carbon
GOPEFB	Gasified oil palm empty fruit bunches
GOPEFBAC	Gasified oil palm empty fruit bunches-based activated carbon
GRTR	Gasified rubber tree root
GRTRAC	Gasified rubber tree root-based activated carbon
hr	hour
IUPAC	International Union of Pure and Applied Chemistry
IR	Impregnation ratio
LM	Langmuir
MG	Malachite green
MPSD	Marquardt's percent standard deviation
MW	Microwave
Min	minute
PFO	Pseudo-first order
PSO	Pseudo-second order
RP	Radiation power

RT	Radiation time
rpm	Rotation per minute
RSM	Response surface methodology
SD	Standard deviation
SEM	Scanning electron microscopy
TGA	Thermogravimetric analyzer
TK	Temkin
TPV	Total pore volume
VM	Volatile matter

**SINTESIS KARBON TERAKTIF DUA FUNGSI DARIPADA SISA
PENGASSAN UNTUK PENJERAPAN PENCELUP HIJAU MALAKIT DAN
ATENOLOL**

ABSTRAK

Lambakan sisa arang gasifikasi yang menyumbang kepada masalah pengurusan sisa pepejal adalah salah satu perhatian utama dalam industri gasifikasi biomas. Kajian ini bertujuan untuk mensintesis karbon teraktif (AC) yang diperoleh daripada sisa pengassan untuk penjerapan pencilup hijau malakit (MG) dan atenolol (ATN) menerusi pengaktifan kalium hidroksida (KOH) dan karbon dioksida (CO₂) menggunakan gelombang mikro teraruh. Keadaan optimum bagi penyediaan semua AC telah ditentukan menggunakan kaedah sambutan permukaan (RSM). Karbon teraktif berasaskan kayu *Glyricidia sepium* yang digaskan (GGSWAC) menunjukkan luas permukaan Brunauer-Emmet-Teller (BET) dan jumlah isipadu liang yang tertinggi sebanyak 633.30 m²/g dan 0.34 cm³/g untuk penjerapan MG; manakala 483.07 m²/g dan 0.26 cm³/g bagi penjerapan ATN. Semua bahan penjerap sangat berpadanan dengan model garis sesuhu *n*-BET yang mencadangkan penjerapan berbilang lapis untuk semua sistem. Karbon teraktif berasaskan akar pokok getah yang digaskan (GRTRAC) dan GGSWAC menunjukkan kapasiti ketepuan maksimum (Q_e) masing-masing sebanyak 259.49 dan 120.57 mg/g, bagi penjerapan MG dan ATN pada suhu 30°C. AC yang digaskan daripada tandan buah kosong kelapa sawit (GOPEFBAC) menunjukkan penyingkiran MG yang agak tinggi dengan nilai Q_e sebanyak 219.39 mg/g. Kajian kinetik menunjukkan bahawa semua sistem mengikuti model Avrami dan langkah yang menghadkan kadar penjerapan MG adalah penyebaran saput, manakala penyebaran saput dan penjerapan kimia mengawal kadar

penjerapan ATN. Kajian termodinamik mengesahkan bahawa semua system adalah tindak balas serap haba melainkan ATN-GRTRAC. Untuk kajian penjerapan di dalam turus lapisan tetap, korelasi terbaik bagi lengkung bulus ditunjukkan oleh model Thomas dan Yoon-Nelson. Keputusan menunjukkan bahawa GGSWAC adalah penjerap yang terbaik kerana prestasi penjerapannya yang tinggi bagi penyingkiran pencelup MG dan ATN.

**SYNTHESIS OF BIFUNCTIONAL ACTIVATED CARBON FROM
GASIFICATION RESIDUES FOR MALACHITE GREEN DYE AND
ATENOLOL ADSORPTION**

ABSTRACT

The abundance of gasification char residues which contributed to solid waste management problem is one of the major concerns in biomass gasification industry. This study aims to synthesize activated carbon (AC) derived from gasification residues for malachite green (MG) dye and atenolol (ATN) adsorption via microwave- induced potassium hydroxide (KOH) and carbon dioxide (CO₂) activation. Optimum preparation conditions for all ACs prepared were determined using response surface methodology (RSM). Gasified *Glyricidia sepium* woodchips-based AC (GGSWAC) showed the highest BET surface area and total pore volume of 633.30 m²/g and 0.34 cm³/g, respectively for MG removal; and 483.07 m²/g and 0.26 cm³/g, respectively for ATN adsorption. All adsorbents best fitted to the *n*-BET isotherm model, suggesting a multilayer adsorption for all systems. Gasified rubber tree root-based AC (GRTRAC) and GGSWAC showed higher maximum saturation capacity (Q_e) of 259.49 and 120.57 mg/g, respectively for MG and ATN adsorption at 30°C. The AC derived from gasified oil palm empty fruit bunches (GOPEFBAC) showed reasonably high removal of MG with Q_e value of 219.39 mg/g. Kinetic studies showed that all system followed Avrami model with film diffusion was the rate-limiting step controlling MG removal, while film diffusion and chemisorption controlled the ATN adsorption. Thermodynamic study confirmed that all systems, except ATN-GRTRAC were endothermic in nature. For the column studies, the better correlation of breakthrough data shown by Thomas and Yoon-Nelson model. Results indicated that

GGSWAC was the best adsorbent due to its high adsorption performance for both MG dye and ATN removal.

CHAPTER 1

INTRODUCTION

1.1 Background of Study

Dyes and pigments, pharmaceutical residues, heavy metals, herbicides, pesticides, oil spillage, fertilizers, pathogens, detergents are among the pollutants presence in the industrial effluents, agricultural runoffs, and domestic discharges (Gupta & Khatri, 2019). Dyes give color to water and create toxic hazards to aquatic ecosystems. The color of dyes hinders the light penetration to water bodies, which could harm the biological processes in the aquatic ecosystem. Pharmaceuticals as emerging pollutants have also become a major concern owing to their low biodegradability, high persistence, and easy bioaccumulation (Zhang et al., 2016). Hospitals, drug factories and households are the main sources of pharmaceuticals waste (Nazari et al., 2016a). The continuous discharge of these pollutants could critically affect aquatic systems and human health (Lu et al., 2016). Hence, these pollutants must be removed from wastewater.

Over the years, numerous technologies such as adsorption, coagulation, flocculation, membrane filtration, chemical oxidation, aerobic and anaerobic degradation, photocatalytic degradation and microbial processes have been used for the wastewater treatment (Qu et al., 2013). Among these technology, adsorption is the most facile, efficient, rapid, and low-cost for pollutants removal (Wong et al., 2018; Yagub et al., 2014). Due to promising advantages offered by adsorption process, it has been widely used for pollutants removal.

1.1.1 Malachite Green

Malachite green (MG) dyes have been commonly used for dyeing of wool, silk and leather, paper, distilleries and food coloring agent (Ayuni et al., 2015). It is also used as bactericide, parasiticide and fungicide in aquaculture industries due to its efficacy and low cost (Oyelude et al., 2018). However, MG is toxic which may cause respiratory destruction, carcinogenesis and mutagenesis. It has been reported that 0.1 mg/L MG released into water bodies can harm the aquatic life and cause detrimental effects in gill, kidney, liver, gonads and intestine (Hidayah et al., 2013). Therefore, the use of MG has been prohibited in aquaculture industries in United States, Canada, the European Union and China. The MG concentration in water has been set in the range of 0.5–100 µg/L according to the environmental quality standard limit (Zhang et al., 2017b). In Malaysia, the maximum allowable limit for dyes has been set to 100 American Dye Manufactures Institute (ADMI) unit according to Environmental Quality Act 1974 (Department of Environment, 2009).

1.1.2 Atenolol

Atenolol (ATN) is among the most prescribed β -blocker drugs, which is commonly used to treat cardiovascular diseases, chest pain as well as hypertension, reduce the probability of heart attacks, and control some forms of heart arrhythmias (Dehdashti et al., 2019). It was reported that half of the administered dose of ATN is excreted via urine, with about 90% still in its active form (Haro et al., 2017). The widespread consumption of ATN as a most prescribed drug and its limited metabolic function in the human body resulted in a large presence of β -blockers in wastewater and surface waters. The ATN concentration in wastewater treatment plant outputs was

predicted to increase from about 0.78 to 6.6 mg/L (Dehdashti et al., 2019), which is greater than the allowable level (10 ng/L) (Hu et al., 2014; Iannuzzi et al., 2009).

Concentration of β -blockers in the surface waters of Europe and North America was found from a few ng/L to 2.2 μ g/L (Alder et al. 2010; Rao et al., 2013), where higher concentrations are measured in the rivers. The measured concentrations of ATN were 1.5–2.6 μ g/L in raw sewages in Switzerland, 0.84–2.8 μ g/L in raw effluent of Spanish wastewater treatment plant, and 1.3 μ g/L in Germany sewage treatment plant (Chang et al., 2019). In Malaysia, 86.6 ng/L of ATN were found in sewage treatment plants effluent around Langat river (Al-Odaini et al., 2013).

Some of the toxic effects of ATN on non-target living organisms include effects on the endocrine glands and the consequent disturbance of testosterone levels in male organisms (Amin et al., 2018). The presence of ATN in the environment has been increased by advancements in the pharmaceutical industry, agricultural development, and ineffective wastewater treatment processes. To reduce the potential risk caused by ATN in water discharged to aquatic environment, their removal is significantly important.

1.1.3 Activated Carbon

Activated carbon (AC) refers to carbon-based materials that possessed high surface area, well-developed porous structure (consisting of pores having diverse size distribution), and broad spectrum of oxygenated functional groups (González-García, 2018). It is well recognized that coconut shells and woods are the most utilized precursors for the large-scale AC production, with a global manufacture of greater than 300,000 tons/year (Mourão et al., 2011). The global AC market size was estimated at USD 4.72 billion in 2018 (Grand View Research, 2019). It is expected to expand (as

shown in Figure 1.1) owing to stringent environmental policies regarding water resources, air quality control and clean gas application (González-García, 2018).

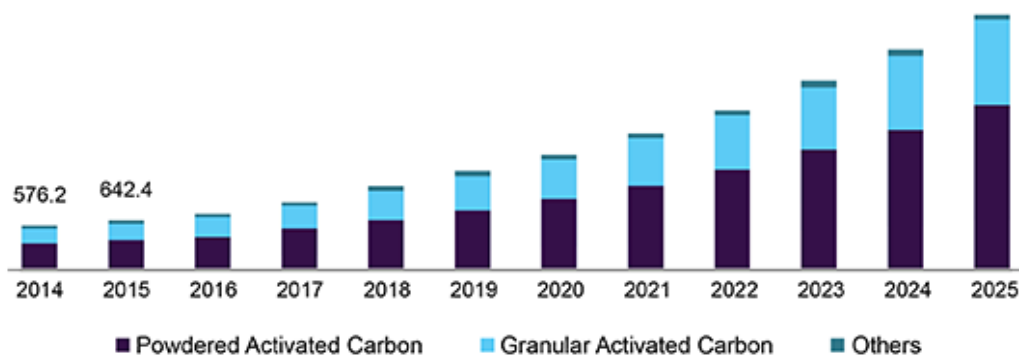


Figure 1.1 U.S. AC Demand 2014-2025 (Grand View Research, 2019)

In 2018, global consumption of AC in water treatment application has reached more than 40% of the total volume manufactured as indicated in Figure 1.2. Due to the excessive demand of AC, there is shortage of precursors such as coconut shell charcoal which are used for making of AC, leading to mounting prices of the raw materials, mainly coconut shell charcoal (Schaeffer, 2011). Besides, the cost of coal-based AC also increased due to the higher demands in other manufacturing industries such as power, iron and steel, and cement industries.

Hence, many studies have been conducted to produce efficient and economical AC from renewable and low-cost resources, such as oak wood (Hajati et al., 2015), coconut pitch (Saman et al., 2015), walnut wood (Ghaedi et al., 2015), rice straw (Sangon et al., 2018), grape pomace (Oliveira et al., 2018), pomelo peel (Low & Tan, 2018), mussel shell (Van et al., 2019), sawdust (Khasri et al., 2018), oil palm waste (Rashidi & Yusup, 2017), orange peel (Pandiarajan et al., 2018), and cotton waste (Sartova et al., 2019; Tian et al., 2019). Most of the studies focused on agricultural waste (Yahya et al., 2015) due to its abundant availability (Tambichik et al., 2018).

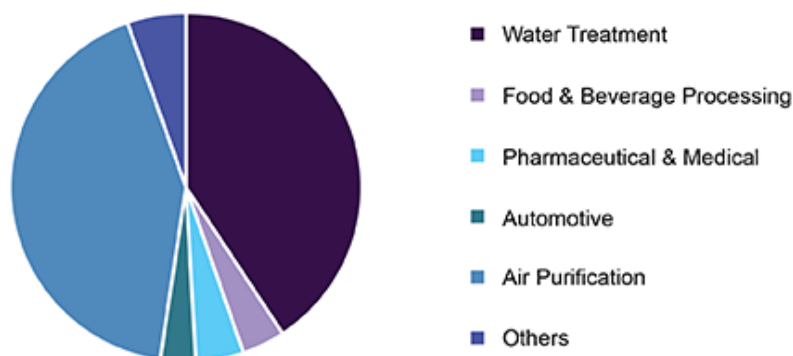


Figure 1.2 Global end use of AC (Grand View Research, 2019)

1.1.4 Gasification Char Residues

Gasification char (GC) is the finer component of the gasifier solid residuals, comprised of unreacted carbon with several amounts of siliceous ash. The irregularly shaped particles have well-developed pore properties and potentially become an excellent adsorbent and precursor for AC production. However, research on its use in adsorption is very rare, despite its high potential as an adsorbent in water and wastewater treatment applications (Jung et al., 2019). Several reported literatures regarding its application in adsorption includes phosphate and nitrate removal (Kilpimaa et al., 2014, 2015), nickel, iron and copper removal (Runtti et al., 2014), rhodamine B removal (Maneerung et al., 2016), congo red and crystal violet removal (Jung et al., 2019), toluene removal (Bhandari et al., 2014) and acetaminophen and caffeine removal (Galhetas et al., 2014a, 2014b).

Depending on type of feedstock, GC possesses a good characteristic as an adsorbent owing to its good porous structure, high specific surface area and enhanced aromatic structure and surface functional groups such as C=O and C–O (Xue et al., 2012).

1.1.5 Microwave Activation Technology

Recently, heating method by microwave (MW) irradiation technology has been progressively applied for the AC preparation. The MW energy is transported to the inner part of the precursors by dipole rotation and ionic conduction, instead of convection and conduction (Makhado et al., 2018). The elimination of pollutant from wastewater using AC developed by MW-assisted activation from numerous precursor such as, empty fruit bunches (Idris et al., 2020), waste palm shell (Nai et al., 2019), corn stalk (Kang et al., 2019), banana peel (Liew et al., 2018), mandarin shell (Koyuncu et al., 2018), rice husks (Ahmad et al., 2018), orange peel (Lam et al., 2017), date stone (Abbas & Ahmed, 2016), coffee shell (Li et al., 2016), almond shell (Du et al., 2016), palm kernel shells (Kundu et al., 2015) and macademia nut endocarp (Pezoti et al., 2014) have been studied by other researchers.

MW heating offers several advantages such as; rapid and efficient energy heating, facile heating control, requires no heat convection through fluid, high char quality (i.e.: pore size and surface area), able to treat waste in-situ and cost effective (G. Li et al., 2016; Wahi et al., 2017).

1.2 Problem Statement

Water pollution has become one of the most serious issues which increases day by day and threatens the sustainability of living organisms. Disposal of synthetic dyes and pharmaceuticals into water bodies such as rivers without proper treatment gives rise to severe problems and concerns. More than 10,000 dyes (Dahri et al., 2014) have been used in textile, paper, cosmetic and food industries, resulting in a large amount of dye wastewater. Apart from dyes, pharmaceuticals also continuously released into the environment in extremely large quantities (Shraim et al., 2017).

MG is one example of dye that can cause various serious problems such as carcinogenesis, mutagenesis, teratogenesis, respiratory toxicity & reduced fertility in humans. Therefore, the use of MG has been banned in several countries and not approved by US Food and Drug Administration or the U.S. Environmental Protection Agency for aquaculture in many countries (Sartape et al., 2017). However, it is still being used as an antiparasitic and antifungal agent in aquacultures due to no insight of the potential genotoxic and carcinogenic properties of MG.

Among several pharmaceutical compounds present in the environment, ATN constitutes one therapeutic class of pharmaceuticals that is not effectively removed from wastewater plant. Limited metabolism by the human body has led to a major part of ATN being non-metabolized during excretion. Studies documented the occurrence of β -blockers in surface water and indicated incomplete degradability of these substances in sewage treatment plant. The presence of these drugs in the aquatic environment can produce toxic effects on non-target species.

Another important environmental issue is the disposal of biomass gasification chars which was generated about 5–10% of the initial feedstock. Presently, gasification char (GC) is treated as waste which is considered as actual loss for the plant owners and no special disposal method has been employed. The growth of gasification industry, which was anticipated to increase up to US \$126 Billion (IMARC Group, 2017) by 2023 will create a substantial increase in solid waste management problem. Hence, it is beneficial to develop the gasification residues as a precursor for AC. To date, there have been no reported studies on MG and ATN removal using carbon residues from biomass gasification plants.

Adsorption process using AC has been considered a superior method for pollutant removals due its high efficiency and operational simplicity. However, this

application is limited by the cost of production and vague methods. The heating techniques for AC production strongly affect its physical and chemical characteristics. The conventional heating, where the heat is transferred to the samples by conduction and convection mechanisms leads to an inhomogeneous heating samples of dissimilar shapes and sizes and requires longer time. Therefore, MW heating technique was used in the present work which can ensure a uniform heating, short activation time and good porosity.

Presently, AC are predominantly synthesized using “one-factor-at-a-time” (OFAT) approach, whereby the desired parameter is varied whilst the other parameters are fixed. Nevertheless, the conventional approach is time-consuming and requires few numbers of experiment, making it unfavourable from the economic point of view. The method also is unable to predict the interaction of parameters with the desired response. Therefore, a useful tool called as RSM were employed for developing, improving and optimizing the preparation condition of AC.

Langmuir and Freundlich models have been widely used to predict the adsorption behavior of pollutant onto adsorbent. However, both models have some limitations. Langmuir model only valid for homogeneous system and ignore the adsorbate-adsorbate interactions, while Freundlich model is only empirical without a theoretical basis and fails at high pressure. Hence, the less explored model such as *n*-BET model was used in this study to predict the adsorption behavior of MG and ATN adsorption on GOPEFBAC, GRTRAC and GGSWAC. In addition, the reports on this model application for MG and ATN adsorption are hardly found.

Fixed bed adsorption offers numerous benefits such as effective removal, facile operation, high capacity, and can be scaled up easily for industrial based on the

information from breakthrough curve. However, there are limited studies in both batch and column mode for MG and ATN adsorption. Therefore, the present work investigates the MG and ATN removal potential using GOPEFBAC, GRTRAC and GGSWAC which are produced via MW-induced KOH activation in both batch and continuous mode of operations.

1.3 Research Objectives

The objectives of the research are listed as follows:

- i. To optimize the ACs preparation conditions using different types of gasification waste (GOPEFBAC, GRTRAC and GGSWAC).
- ii. To evaluate the physical and chemical properties of the optimized ACs.
- iii. To assess the influence of contact time, initial solution concentration, temperature and pH on MG and ATN adsorption in batch adsorption mode.
- iv. To analyze the adsorption isotherm, kinetic, mechanism and thermodynamic of MG and ATN adsorption.
- v. To evaluate the effect of influent solution concentration, bed depth and feed flow rate on breakthrough curves in continuous adsorption mode.

1.4 Scope of Study

There are several scopes to be focused in detail in order to attain the project objectives. The scopes of study are outlined as follows:

- i. GOPEFB, GRTR and GGSW were converted into ACs via MW induced KOH-CO₂ activation. The variable process parameters involved radiation power (264 - 616 W), radiation time (1 - 8 min) and impregnation ratio (0.5 - 2) were optimized to maximize the yield of AC and their adsorption performance for MG and ATNs removal using RSM adopting central composite design (CCD).
- ii. The optimized ACs were characterized in terms of surface area, pore characteristic, surface morphology, proximate content, elemental composition and surface chemistry. For batch mode, the influence of contact time (0 - 24 hours), initial concentration (50 - 300 mg/L), solution temperature (30 - 60 °C) and initial solution pH (2 - 12) on adsorption efficiency were evaluated.
- iii. Freundlich, Langmuir, Sips, Dubinin–Radushkevich, Temkin, and *n*-BET models were employed in isotherm studies, while Pseudo-first order, Pseudo-second order, Avrami and Elovich were evaluated in kinetic studies, and Weber-Morris intraparticle diffusion (IPD) model, Boyd's plot and diffusion-chemisorption models were examined to determine the rate-limiting step of the MG and ATN adsorption systems. The thermodynamic parameter such as ΔH , ΔS and ΔG were estimated.
- iv. The effects of various continuous adsorption parameters, including initial feed concentration (100 - 200 mg/L), feed flow rate (0.5 - 2 mL/min), and

bed depth (1-3 cm) were investigated. The breakthrough curves were plotted and evaluated using three model equations which are Adams–Bohart, Yoon–Nelson and Thomas.

1.5 Gap of knowledge

The application of gasification char residues in adsorption field for the removal of MG and ATN has not yet been explored. Therefore, the main goal of this study is to synthesis the bifunctional ACs for MG and ATN adsorption.

1.6 Thesis Outline

This thesis is structured into five chapters and summarized as follows:

Chapter 1 comprises of the research background, problem statement, research objectives and scope of study.

Chapter 2 gives a review of literature pertaining to pollutant and toxicity, regulation and pollutant removal techniques. The fundamental of AC adsorption, activation process, MW heating and optimization using RSM are outlined. Adsorption isotherm, kinetics, mechanism and thermodynamics are also been highlighted in this chapter. The last section explains the breakthrough modeling for fixed-bed column studies.

Chapter 3 describes in detail all the materials and equipment used in the present study. The experimental set up and experimental procedure which include the preparation of AC, design of experiments, batch and continuous process are also included.

Chapter 4 is divided into four sections which are (i) experimental design and optimization results, (ii) characterization results, (iii) batch adsorption studies, and (iv) continuous adsorption studies

Chapter 5 concludes the findings from this study. Several recommendations are presented for upcoming research works.

CHAPTER 2

LITERATURE REVIEW

2.1 Introduction

This section reviews the previous findings reported by other researchers on adsorption, GC properties, AC production, optimization of AC preparation using MW irradiation, effect of parameter on batch adsorption study, adsorption isotherm and kinetic study, adsorption mechanism, thermodynamics properties of adsorption and fixed-bed column studies.

2.2 Adsorption

Adsorption is a mass transfer process whereby elements gather at the interface of two different phases, such as gas-solid and liquid-solid (De Gisi et al., 2016; Xue et al., 2012). The adsorbed substance is called adsorbate, while the substance used to adsorb the adsorbate is called adsorbent. Adsorption can be either a chemical (chemisorption) (Aljeboree et al., 2017) or/and physical (physisorption) process (Toumi et al., 2018). Generally, for physisorption, the attractive forces between the adsorbate molecules and adsorbent are Van der Waals forces, which are weak in nature and result in reversible adsorption. On the other hand, if the attraction forces are due to chemical bonding, the adsorption process is called chemisorption. Chemisorption is characterized by the formation of strong chemical associations between the molecules or ions of adsorbate and the adsorbent surface, which are generally due to the exchange of electrons between them and thus, chemisorption is generally irreversible. In general, the adsorption process involves both chemical and physical adsorption.

Adsorption has been determined to be superior to other pollutants removal techniques owing to its flexibility and simplicity of design, high efficiency, insensitivity to toxic pollutants, and ease of operation compared to other removal techniques such as membrane separation, ion exchange, coagulation/flocculation, chemical oxidation, electrochemical, photochemical and biodegradation.. Table 2.1 summarizes the advantages and disadvantages of various pollutant removal methods.

Table 2.1 Advantages and disadvantages of various pollutant removal technologies (Zhou et al., 2019)

Technology	Advantages	Disadvantages
Adsorption	High efficiency, offer excellent quality of the treated effluent, simple operation (simple equipment, adaptable to many treatment process)	Ineffective to certain pollutants, issues on the disposal of adsorbent residues (elimination of the adsorbent requires incineration, regeneration or replacement of the material).
Membrane separation	Small space requirement, simple, rapid and efficient even at high concentrations	Investment costs are often too high for small and medium industries, high energy requirements, high maintenance and operation costs.
Ion exchange	Rapid and efficient process	Ineffective for certain target pollutants (disperse dyes, drugs, etc.), performance sensitive to pH of effluent, require regular inspection and unloading and loading of new exchange resins, which are disruptive to operations and mean ongoing operational costs
Coagulation/ Flocculation	Rapid and efficient for insoluble contaminants (pigments, etc.) removal	High sludge production and disposal issues, requires accurate chemical dosing (this may be an unsuitable wastewater treatment method if the inlet water quality fluctuates often

Table 2.1 Continued

Technology	Advantages	Disadvantages
Advanced oxidation process	High efficiency, rapid	Sludge production, economically unfeasible, high chemical reagents and electricity consumption, formation of by-products
Electrochemical process	High efficiency (more effective and rapid organic matter separation than in traditional coagulation), does not require the addition of chemical reagents	High initial cost of the equipment, high electricity consumption
Photochemical process	No sludge production, rapid	The formation of by-products and power consumption
Biodegradation	Economically attractive and simple	Require strict external environmental conditions, slow process, occupy a certain area of land

2.3 Gasification Char Residues as a Precursor for AC Production

Gasification is the conversion of carbonaceous material into a gaseous product or synthesis gas that mainly consists of hydrogen and carbon monoxide, with lower amounts of carbon dioxide, water, methane, higher hydrocarbons and nitrogen in the presence of a gasifying agent (for example air, pure oxygen, or steam, or mixtures of these components) at temperatures between 500 and 1400 °C (A. A. Ahmad et al., 2016). Meanwhile, gasification char (GC) is unreacted carbonaceous solid residue obtained after gasification process. The physical and chemical properties of char are significant to determine its potential application. In adsorption, the removal efficiency and pore characteristics of the adsorbent depend on its physical and chemical properties. In this section, the chemical and physical characteristics of GC obtained from the existing literature were reviewed.

2.3.1 Physical Properties

Specific surface area, total pore volume and average pore diameter of char are among the important features of char that influence the adsorption efficiency. The specific surface area is a ratio of the total pore surface area to the total char particle mass. (You et al., 2017). The pore size influences the accessibility of the active sites and mass transfer. Based on the International Union of Pure and Applied Chemistry (IUPAC), micropores, mesopores, and macropores are classified as pores with diameter <2 nm, 2-50 nm, and >50 nm, respectively (Cha et al., 2016; Tan et al., 2015). The different pore sizes can be expected to exhibit different behaviour during adsorption as pressure increases. The sorption behaviour in micropores is generally controlled by the interactions between fluid molecules and the pore walls. Meanwhile, the sorption behaviour in mesopores not only depends on the fluid-wall attraction, but also on the interactions between the fluid molecules itself, which results in the formation of multilayer adsorption and capillary condensation (Thommes, 2010).

Previous researchers have evaluated the physical properties of GC based on different biomass types, various equivalence ratio and temperature. For example, Hernández et al., (2016) studied the effect of the main gasifier operating conditions on the properties of char produced using small-scale drop-tube pilot plant gasifier. They reported that an increase of the relative biomass/air ratio results in a higher production of more aromatic and stable char; and the increase in carbonisation reaction extent. However, they found that all the obtained chars have low specific surface area (less than $70 \text{ m}^2/\text{g}$), which is not suitable for adsorption application without further activation. In another study, GC from straw gasification was reported to have high surface area of $1027 \text{ m}^2/\text{g}$ (Hansen et al., 2015). Similarly, Zhai et al. (2017) also reported high surface area of sawdust GC with the value between 948.84 and 987.61 m^2/g , as temperature

were increased from 800 °C to 1000 °C in steam atmosphere, owing to the rise of carbon conversion.

Lundberg et al. (2016), who studied the effect of fuel size and surrounding conditions on the rate of biomass gasification in a laboratory-scale bubbling fluidized discovered that the specific surface area of the GC differed from 469 to 1581 m²/g, subjected to different boundary conditions. Meanwhile, Dias et al. (2017) compared the characteristics of chars from the gasification and pyrolysis of rice waste streams towards their potential as adsorbent materials. They reported that GC have higher surface areas which is between 26.9 to 62.9 m² g⁻¹, while pyrolysis chars contain no porous matrix, due to high volatile matter content. They concluded that the GC possessed adequate properties that could be developed as adsorbent while the pyrolysis chars need to be further activated.

The activated GC will generally have higher specific surface area. This is proven by Maneerung et al. (2016), who prepared AC from woody biomass gasification for dye adsorption. They reported that the char has high surface area after steam activation at 900 °C. The specific surface area was discovered to have significant increment from 172 to 776 m²/g, which has high dye adsorption capability. In a nutshell, the GC properties were vary among the samples depending on the combination of gasification technology, temperature, gasification agent and initial feedstock (Benedetti et al., 2017). Table 2.2 summarizes the physical characteristic of GC reported in the literature.

From the previous findings, it is concluded that the chars with high S_{BET} and total pore volume were gasified at high temperature and steam as gasifying agent. The GC has a specific surface area and pore volume range from 2 to 1581 m²/g and 0.002 to 0.657 cm³/g, respectively which are comparable with the AC that has surface area and pore volume range from 500 to 2000 m²/g and 0.20 to 0.60 cm³/g respectively

(Marsh & Rodríguez-Reinoso, 2006). These chars are suitable to be developed as low-cost adsorbent, as it is much cheaper with low energy requirements (no carbonization step in AC production). Moreover, the feedstocks of GC production are abundant (1300 tonne/year) (Benedetti et al., 2019), mainly obtained from biowastes.

2.3.2 Chemical Properties

Chemical characteristic such as carbon and ash contents, functional groups, pH and aromaticity are significant for adsorption. Char with high carbon content (50-90%) is suitable to be produced as AC for adsorption (Danish & Ahmad, 2018). Data on functional groups give information on the possible interactions between adsorbent and adsorbate. Carboxylic acids, anhydrides, lactones, lactols, and phenols, are acidic, while carbonyl and ether groups are neutral. Basic functionalities are presented by quinone, chromene, pyrone and nitrogen groups (Rivera et al., 2011; Shafeeyan et al., 2010). For ACs and chars, greater amounts of oxygen-containing surface functional groups (especially carboxyl) result in enhanced sorption of metal ions in controlled aqueous media (Uchimiya et al., 2011).

The GC was reported to have higher ash content (40.4-64.07%) and lower moisture (0.69-3.4%) and fixed carbon content (21.98-40.49%) at high equivalence ratio (Qian et al., 2013). The char surface functional groups varied between the types of biomass feedstock. Ducouso et al. (2015) reported that phenol, ether and quinone were the dominant O-containing functions on the surface of wood chip GC.

GC generally poses low functional groups due to significant loss of functional groups such as hydroxyl, carboxyl, and carbonyl at high gasification temperature (Wiedner et al., 2013), but it also depends on the feedstock of the char.

Table 2.2 Physical characteristic of GC residues

Feedstock	Types of Gasifier	Gasifying Agent	Temperature (° C)	S _{BET} (m ² /g)	Pore volume (10 ⁻³ mL/g)	Reference
Switchgrass Sorghum Red cedar	Fluidized bed	Air (ER =0.28) Air (ER =0.28) Air (ER =0.25)	700-800	21 5.6 61	11.88 2.14 31.33	(Qian et al., 2013)
Wheat straw pellet Pine wood Sieved pine wood	Circulating fluidized bed Two stage gasifier	Steam	750 1000-1200	75 1027 426	40 580 520	(Hansen et al., 2015)
Dealcoholized marc of grape	Entrained flow	Air Steam	1200 1200	60 35	N/A	(Hernández, et al., 2016)
Activated mesquite wood chips	Downdraft fixed-bed	N/A	N/A	776	657	(Maneerung et al., 2016)
Soft wood chips Soft wood pellets	Bubbling fluidized bed	Steam	850	489 1581	N/A	(Lundberg et al., 2016)
Sawdust	Fixed bed reactor	Steam-Air	800-1000	945-988	N/A	(Zhai et al., 2017)
Rice husk & polyethylene mixture	Bubbling fluidized bed	Steam-Air	850	27-63	N/A	(Dias et al., 2017)

Table 2.2 Continued

Feedstock	Types of Gasifier	Gasifying Agent	Temperature (° C)	S _{BET} (m ² /g)	Pore volume (10 ⁻³ mL/g)	Reference
Wood chips	Downdraft	Air	~650	352	240	(Benedetti et al., 2017)
Pellets	Rising co-current	Air	~700	128	180	
Wood chips	Downdraft	Air	~650	78	80	
Wood chips	Downdraft	Air	~800	281	130	
Wood chips	Dual-stage gasifier	Air	~900	587	300	
Wood chips	Dual-stage gasifier	Air	~850	272	150	
Pine wood	N/A	N/A	600-900	N/A	N/A	(Marks et al., 2016)
Switchgrass	Downdraft	N/A	N/A	64	90	(Bhandari et al., 2014)
Switchgrass	Fluidized bed	N/A	N/A	2	20	
Pine wood	Updraft	Air	1000	183	70	(Huggins et al., 2015)
Poplar Wood	Fluidized bed	Steam	750	573.8	219	(Ducousso, et al., 2015)

A higher O/C ratio in a char material may indicate the presence of more functional groups (i.e: hydroxyl, carboxylate, and carbonyl) that could contribute to a higher cation exchange capacity (CEC) value (Yuan et al., 2011) due to higher negative charge surface of the chars, which could facilitate the adsorption through electrostatic attraction between the positively charged pollutant and negatively charged char surfaces (Xu et al., 2011).

The high degree of carbonization, which removes acidic functional groups of the feedstock, making the char surface become basic (Shen et al.,2016). The GC pH generally falls into the alkaline range ($7 < \text{pH} < 12$) depending on the feedstock (Griffith et al., 2013; Hansen et al., 2016). This basic characteristic of char was due to low amounts of oxygen groups presence, which was responsible for electrostatic interaction between positively charged char with negatively charge pollutants. GC also had a higher degree of aromatic carbon (Abdulrazzaq et al., 2014) at high temperature (Kraft et al., 2018; Wiedemeier et al., 2015) indicating its high chemical stability, which is suitable for adsorption application.

In conclusion, char characteristic such as porous structure, high specific surface area, enriched surface functional groups and minerals make it suitable to be an adsorbent for pollutants removals (Prasara-A & Gheewala, 2017; Shen & Fu, 2018). The oxygen-rich functional groups including C=O and C–O, and aromatic groups on GC can possibly act as strong active sites and improve the char's adsorption performance (Xue et al., 2012). Table 2.3 summarizes the chemical composition of GC.

Table 2.3 Chemical properties of GC

Feedstock	Technology	Gasifying Agent	Temperature (° C)	Fixed Carbon (%)	Ash (%)	Reference
Switchgrass	Fluidized bed	Air (ER = 0.20, 0.25, 0.28)	700-800	34.99	51.61	(Qian et al., 2013)
Sorghum				33.76	50.89	
Red cedar				40.49	40.41	
Pine wood	N/A	N/A	600-900	79.34	10.79	(Marks et al., 2016)
Switchgrass	Downdraft	Air	N/A	64.80	N/A	(Bhandari et al., 2014)
Switchgrass	Fluidized bed	Air	N/A	1.38	N/A	
Pine wood	Updraft	Air	1000	N/A	N/A	(Huggins et al., 2015)
Poplar wood	Fluidized bed	Steam	750	77.40	3.60	(Ducouso et al., 2015)
Corn stover	Fluidized bed	Steam	850	42.00	47.10	(Cheah, et al., 2014)
Oak				76.9	N/A	

2.3.3 Recent Studies on Adsorption Using GC

Contrarily to other materials used for adsorption studies, the use of gasification residues is scarcely found in the literature. The literature regarding its application in adsorption is somewhat limited to heavy metals and tar removal. Only few researchers reported the dye and pharmaceutical adsorptions utilizing GC as adsorbent or precursor for AC. For instance, Maneerung et al., (2016) investigated the removal Rhodamine B (RhB) using AC from gasification of mesquite wood chips in downdraft fixed-bed gasifier. They reported that the prepared AC exhibited high RhB adsorption capability. This was owing to its high specific surface area (776.5 m²/g) and the abundance of

carboxyl and hydroxyl groups. They also discovered that the experimental data well fitted Langmuir model with the maximum monolayer adsorption capability of 189.8 mg/g. They concluded that the utilization of GC as a precursor of AC lowers the AC production cost; offers a cost effective and environmental friendly measures in recycling char; and lessening the environmental problems related to its disposal. Meanwhile for pharmaceutical adsorption, Galhetas et al. (2014a) used activated pine gasification residue with K_2CO_3 treatment for adsorption of acetaminophen. They also used gasification residue of pine and coal for caffeine and acetaminophen adsorption from aqueous solutions (Galhetas et al., 2014b). It was found that the activated pine produced porous materials that aid the acetaminophen and caffeine removal, which was controlled by the micropore size distribution of the AC. They concluded that the surface chemistry appears to be the determining factor that rules the interaction of caffeine and the AC.

Other researchers reported the use of GC for heavy metal removals. The activated char from pine and spruce gasification have been used for removing nitrate and phosphate (Kilpimaa et al., 2014, 2015). Both physical and chemical activation was conducted using char from a downdraft and physical activation by CO_2 at high temperature was found to be the most effective process. The maximum monolayer adsorption capability (q_m) of activated char for phosphate and nitrate was 80 and 20.5 mg/g, respectively. Similar type of char (pine & spruce) was used by Runtti et al. (2014) who studied the adsorption of iron, copper and nickel. They gasified the wood chips at a rate of 50 kg h^{-1} in a 150 kW downdraft gasifier, operating at $1000 \text{ }^\circ\text{C}$. They found that the removal of metals by GC with and without chemical activation was 2-5 times greater than commercial AC. The highest maximum experimental sorption capacities ($q_{m,exp}$) for iron, copper and nickel by GC were 21, 23 and 18 mg/g, respectively. They

concluded that the GC (with and without chemical activation) could be utilized in wastewater treatment due to their high adsorption efficiency.

The GC derived from switchgrass has been found to have high toluene removal efficiency (Bhandari et al., 2014). The activated char resulted in higher toluene removal efficiency (92%) compared to the raw char from gasifier (79%). This is explained by the texture of the char particles, which were closed and not porous due to the unburnt volatiles, while the activated char showed clear pore developments resulting in larger surface area ($\sim 900\text{m}^2/\text{g}$). Godinho et al. (2017) analyzed the efficiency of chars obtained from the gasification and co-pyrolysis of rice wastes, as adsorbents of Cr^{3+} from aqueous solution. They concluded that GC is very efficient to remove Cr^{3+} from aqueous solution which requires no further activation. Similar study was conducted by Dias et al. (2018) who found that the rice waste chars from the steam-oxygen gasification gave higher Cr^{3+} adsorption efficiencies and uptake capacities than commercialized AC. Table 2.4 summarizes the findings from literature regarding the adsorption application from GC residue.

2.4 AC Production

AC refers to a carbonaceous adsorbent with a highly amorphous structure and a highly developed internal pore structure. It has been proven to be a superior adsorbent for the elimination of numerous pollutants from gaseous or aqueous media. It is extensively used due to its high surface area ($500\text{-}1500\text{m}^2/\text{g}$), well-developed internal microporosity (a pore size distribution of $<1\text{-}100\text{ nm}$), and broad range of surface functional groups (carboxylates, carbonyls, hydroxyls, amines) (Pallarés et al., 2018; Rivera et al., 2011). These properties give AC an exceptional ability to adsorb a wide variety of molecules (Benedetti et al., 2017).